A model for co-clusters and their strengthening in Al–Cu–Mg based alloys: a comparison with experimental data

Marco J. Starink

Materials Research Group, Engineering Sciences, University of Southampton, Southampton, UK

A model for the thermodynamics of and strengthening due to Cu–Mg co-clusters in Al–Cu–Mg based alloys is analysed and tested. The formulation uses a single interaction enthalpy between dissimilar alloying elements (e.g. Cu and Mg atoms in an Al–Cu–Mg based alloy) combined with the configurational entropy. The metastable solvus in Al–Cu–Mg based alloys is calculated. Recently published small angle X-ray scattering experiments, 3 dimensional atom probe and yield strength data on these type of alloys support the model. The small angle X-ray scattering and hardness experiments, as well as calorimetry experiments, are sensitive to the main free energy (or enthalpy) changes, which are dominated by Cu–Mg bonds formed by the dimers and the local electron densities related to these bonds. 3 dimensional atom probe is less sensitive to dimers, and will detect agglomeration of dimers to form larger clusters.

1. Introduction

In many alloys the strengthening is predominantly due to stable or metastable second phases which act as obstacles to dislocation motion. In particular, all medium to high strength Al alloys are strengthened predominantly by stable or metastable second phase precipitates or clusters. Metastable second phases can be very small: precipitates as small as 2 to 10 atoms have been proposed [1, 2]. These small precipitates are effectively formed from a metastable solution through a solute clustering process. If the clusters formed involve two alloying elements, the term co-clusters is employed; the simplest form of a co-cluster is a pair of neighbours of dissimilar alloying atoms termed a dimer. If the pair is in nearest neighbour position, we can term it a nearest neighbour dimer.

A theory for the thermodynamics of co-clusters in metallic alloys and the strengthening caused by them was presented recently [3]. Since the publication of that work new experiments on the formation of Cu–Mg co-clusters in Al–Cu–Mg based alloys have been published [1, 2, 4, 5, 6]. The objective of the present paper is to review the basic elements

and assumptions in the model, to present some new predictions of the model and to compare the model and its predictions to recently published data.

Al–Cu–Mg alloys, which are the topic of the present work, are widely used in structural aerospace applications due to their good combination of specific strength and damage tolerance [7]. Age hardening of Al–Cu–Mg alloys with composition in the (α+S) phase field occurs in two distinct stages separated by a constant hardness plateau, see Fig. 1 (data from [8, 9]). The first stage of hardening is attributed to the formation of Cu–Mg co-clusters and the second stage is generally attributed to the precipitation of the S (Al_2CuMg) phase [4, 10, 11, 12].

2. Model for co-clusters, their thermodynamics and metastable phase diagram

The model is built up from considering the smallest co-cluster possible, which is a dimer. The solvi of the co-clusters in the ternary system can be derived as follows. Consider alloying elements A and B (in our case Cu and Mg) in a host metal M (in our case Al), the total number of the respective elements in the system are N_A, N_B and N_M. The Gibbs free energy, G, of the system can be approximated as [3]:

$$G = H_o - N_{cl}\Delta H_{A-B} - TS \tag{1}$$

where N_{cl} is the number of A–B dimers, H_o is a constant reference enthalpy, S is the entropy and ΔH_{A-B} is the enthalpy of formation of an A–B dimer from the random solution, i.e. the enthalpy of the reaction in which one A atom and one B atom, originally in random solution, form an A–B dimer.

The entropy of the system is proportional to the logarithm of the number of states w in the system. If we consider the dimer to be a nearest neighbour dimer then it follows [3]:

$$S = k_B \ln w = k_B \ln\left(\frac{N!}{(N_M!(N_A - N_{cl})!(N_B - N_{cl})!12N_{cl}!}\right) \tag{2}$$

where k_B is Boltzmann's constant. For equilibrium it holds $\partial G/\partial N_{cl} = 0$. Performing this derivation using the latter two equations (using the Stirling approximation $\ln N! = N\ln N - N$) then provides that at equilibrium [3]:

$$c_A c_B = \exp(-2)\exp\left[\frac{-\Delta H_{A-B}}{RT}\right] \quad (3)$$

where c_A is the solubility (i.e. the equilibrium molar fraction) of element A in the M rich host lattice, c_B is the solubility of element B in the M rich host lattice.

In Ref. [3], ΔH_{A-B} for Cu–Mg co-clusters was determined and verified through measurements of enthalpy changes on co-cluster formation using calorimetry. This provided $\Delta H_{A-B} = 34.5 \pm 0.5$ kJ mol^{-1}. The metastable solvus of co-clusters in the Al–Cu–Mg phase diagram determined through Eq. (3) is presented in Fig. 2.

It should be noted that c_A and c_B as used in Eq. (3) refer to compositions of alloying elements that are available for cluster formation. In commercial purity Al–Cu–Mg based alloys and Al–Cu–Mg alloys with solute contents close to the solvus, some of the Cu and Mg in the alloy will not be available because these elements are incorporated in undissolved intermetallic phases. For instance, in Al-2024 $Al_{20}Cu_2Mn_3$ (the T phase dispersoids), $Al_7Cu_2(Fe,Mn)$ and Al_2CuMg (S phase) is present, with smaller amounts of $Al_{12}(Fe,Mn,Cu)_3Si$ (cubic alfa phase) and $AlCu_2$ (theta phase) [11, 13, 14].

Taking the latter into account, the typical amounts of alloying elements available for co-cluster formation in Al-2024 is 1.5at.%Mg and 1.5at.%Cu, which provides a solvus temperature of 380 ºC. (This may seem a high temperature, but it should be noted that because the stable S phase forms very rapidly at these temperatures co-clusters can only be present for a few seconds, and detecting them will be extremely challenging. Thus co-cluster formation tends to be only relevant at low temperatures, where formation of stable phases is slow.)

3. Model for strengthening due to co-clusters

As shown in [3] strengthening due to (short range) order is by far the most important strengthening effect for Cu–Mg co-clusters. (The secondary strengthening effect, modulus hardening, amounts in most cases to about 10 % of the total strengthening effect.) The strengthening due to an ordered phase which contains short or long range order depends on the way the dislocations interact with the precipitate or clusters. For co-cluster strengthening, the order can be considered to be extremely short ranged. In the model [3] we consider that the work done in deforming the lattice through movement of dislocations hampered by (co-)clusters equals the change in energy related to the short range order per unit area on slip

planes. We consider co-clusters consist of a single pair of atoms A and B. The amount of A atoms in the co-clusters is y_A, the amount of B atoms in the co-clusters is y_B. The amount of A atoms in the matrix is x_A, the amount of B atoms in the matrix is x_B. Through considering the geometry and nearest neighbour constellations in the fcc lattice it can then derived that the increment in critical resolved shear stress due to the SRO effect is given by [3]:

$$\Delta\tau_{\mathrm{SRO}} = \frac{\gamma_{\mathrm{SRO}}}{b} = \frac{\Delta H_{\mathrm{A-B}}}{b^3}\frac{4}{\sqrt{3}}\left(\frac{2}{3}(y_{\mathrm{A}} + y_{\mathrm{B}}) - \left(\frac{2}{3}y_{\mathrm{A}}x_{\mathrm{B}} + \frac{2}{3}y_{\mathrm{B}}x_{\mathrm{A}} + 2x_{\mathrm{A}}x_{\mathrm{B}}\right)\right) \tag{4}$$

where b is the Burger's vector, and γ_{sro} is the change in energy per unit area on slip planes on the passing of one dislocation (a.k.a. the diffuse interphase boundary energy [15]). The latter expression provides the dominant strengthening mechanism in Al–Cu–Mg alloys containing Cu–Mg co-clusters [3]. For dilute alloys x_A , x_B, y_A, y_B << 1 and we can approximate the latter equation as:

$$\Delta\tau_{\mathrm{SRO}} \cong \frac{\Delta H_{\mathrm{A-B}}}{b^3}\frac{8}{3\sqrt{3}}\left(y_{\mathrm{A}} + y_{\mathrm{B}}\right) \tag{5}$$

This shows that the strengthening effect is in good approximation proportional to the amount of co-clusters formed (see discussion).

A full model for prediction of the strength of the alloy including secondary strengthening mechanisms such as modulus hardening and solution hardening is provided in [3].

Examples of predictions of strength of Al–Cu–Mg alloys with the above model in combination with solution strengthening and modulus strengthening (see [3]) are presented in Figs. 3 and 4. Figure 3 shows predictions of strength of Al–Cu–Mg alloys aged at 120 °C. Figure 4 shows strength predictions for alloys aged at 20 °C.

4. Comparison of model predictions with data

Substantial data on Cu–Mg co-clusters obtained through three dimensional atom probe (3DAP) experiments, X-ray scattering experiments and calorimetry have recently been published [1, 2, 3, 4, 5], and strength and hardness evolution due to co-cluster formation has been determined in various studies [2, 6]. It is noted that whilst 3DAP studies have been crucial in identifying the existence of co-clusters from the mid-1990s there are limitations to the capabilities 3DAP in determining composition and size of the smallest co-clusters. The

root cause for this is that detection rate of alloying elements are on average around 50 % [2]. This limitation will cause 75 % of any dimers present to go undetected. In general, the possibility of non-detection of clusters and misidentification of cluster type in 3DAP due to non-detection of atoms is quite complex owing to factors such as size (number of atoms) and morphology of the cluster detected by the cluster-finding algorithm [2]. For example, two Cu–Mg dimers located 0.4 nm apart may be identified in a large number of ways depending on detection or non-detection of individual atoms and setting of parameters in the cluster-finding algorithm. Identification as a cluster with 3 alloying elements and Cu:Mg ratio 1:2 or 2:1, as a Cu–Cu cluster, a Mg–Mg cluster, or a single Cu–Mg dimer are all possible, with very similar probabilities.

4.1. Size of co-clusters

The model considers that the smallest unit of a co-cluster is the dimer, and particularly the case for a pair of nearest neighbours of dissimilar alloying atoms is considered. The effective dimensions of a nearest neighbour dimer in the 3 orthogonal directions is b, b and $2b$ i.e. for fcc aluminium this is ~0.29 × 0.29 × 0.58 nm. Recent in-situ small-angle X-ray scattering (SAXS) experiments on an Al-2.5Cu-1.5Mg (wt.%) alloy during ageing at 200 ºC shows a Guinier radius of clusters of 0.45 nm [4], corresponding well with 1 to 2 Cu–Mg nearest neighbour dimers. SAXS is sensitive mainly to local electron density and should thus be primarily sensitive to the bonds that cause the main changes in free energy in the material. The present model incorporates a single interaction enthalpy, and hence there is no significant driving force for growth of the co-clusters. The model effectively assumes that the configuration of electrons and the energy of the system is determined by the creation of Cu–Mg bonds, and any further reorganisation, for instance by formation of larger clusters, would have relatively little effect on configuration of electrons and the energy of the system. This corresponds with the in-situ small-angle X-ray scattering experiments which show that the effective Guinier radius of the co-clusters is constant for an extensive period during the initial stage of ageing in which the hardness is constant [4]. (Subsequent increase in Guinier radius [4] is due to the formation of S phase precipitates.)

Through a cluster identification algorithm dimers are detected in 3DAP data on Al–Cu–Mg alloys. However, these algorithms also detect larger clusters for which Al content is generally much larger than solute atom content [1, 2, 16].

These findings of SAXS, 3DAP and hardness experiments are consistent with the present model. The SAXS and hardness, as well as calorimetry experiments [3, 16], are essentially sensitive to the main free energy (or enthalpy) changes, which are dominated by Cu–Mg bonds formed by the dimers. 3DAP is less sensitive to dimers, and will mainly detect agglomeration of dimers to form larger clusters, but this agglomeration process is related to smaller changes in free energy (or enthalpy) causing no change in hardness.

4.2. Composition of co-clusters

The model considers that the effective composition of a co-cluster is 50 % Cu and 50 % Mg. The observation that a comparison of resulting predictions with calorimetry data on enthalpy changes on 10 alloys with a wide range of Cu:Mg ratios show a good agreement [3], is a first indication that this assumption on the Cu:Mg ratio in the clusters is correct. Recent analysis of 3DAP experiments on an Al-2024 alloy aged at 170 °C for 0.5 h using a cluster identification algorithm shows co-clusters with Mg:Cu ratio of the solute clusters of 1.15 [1] with an Al content of ~91 %. Similar analysis of Al-1.1Cu-0.2Mg and Al-1.1Cu-0.5Mg alloys after ageing at 150 °C for 0 s (i.e. as-quenched), 60 s and 1 h shows Mg:Cu ratios around 0.5 to 2, whilst for an Al-1.1Cu-1.7Mg (at.%) alloy aged at 150 °C for 0 s (i.e. as-quenched), 60 s and 1 h shows Mg:Cu ratios close to 1 [2]. Considering that detection efficiency in a 3DAP apparatus is always less than 50 %, these data compare well with the assumptions in the model.

4.3. Amounts of co-clusters formed

From in-situ small-angle X-ray scattering experiments on an Al-2.5%Cu-1.5%Mg (wt.%) alloy during ageing at 200 ºC Deschamps et al. [4] concluded that the amount of co-clusters formed is about 2 vol.% (with a likely range of 1.2–3.5 %). For that alloy the present model predicts the total amount of co-clusters (in the form of Cu–Mg dimers) to be 1.6 at%.

4.4. Strength and hardness predictions

Since publication of [3] several data on yield strength and hardness of co-cluster strengthened high purity Al–Cu–Mg alloys have been published [2, 6, 17]. This data is compared with model predictions in Table 1 and in Fig. 5. (Vickers hardness data is converted to yield strength using the proportionality relation determined for a similar Al–Cu–Mg alloy with

similar strength in [18]: σ_y = 2.5 × HV). Figure 5 shows model predictions correspond closely with measured data.

The model retains a very high accuracy up to measured yield strengths of about 350 MPa, and shows some limited scatter beyond these strength levels. For these high strengths it needs to be considered that the corresponding alloys will have Cu and Mg contents that are very close to the solvus at the solution treatment temperature. Strength will be influenced strongly by the amount of undissolved Cu and Mg containing phases (particularly S phase) which in turn can be influenced by prior processing and the occurrence of any macrosegregation. Hence improvement in prediction of these strengths would require a detailed model of solution of intermetallic phases incorporating prior processing, which is at present not included. Thus the limited scatter at higher strengths is unlikely to be related to the details of the cluster strength model.

Alloy	Ageing temperature (ºC)	HV measured (HV)	σ_y measured (MPa)	σ_y model (MPa)	Source
Al-2.5wt%Cu-1.5wt%Mg	200		210	227	[6]
Al-1.1at%Cu-0.5at%Mg	150	70	175	156	[2]
Al-1.1at%Cu-0.75at%Mg	150	80	200	189	[2]
Al-1.1at%Cu-1at%Mg	150	92	230	217	[2]
Al-1.1at%Cu-1.7at%Mg	150	102	255	257	[2]
Al-3.8wt%Cu-1.3wt%Mg-0.05wt%Fe	175	127	317	317	[17]

Table 1 Vickers hardness (HV) and yield strength for high purity Al–Cu–Mg alloys aged to the hardness plateau due to Cu–Mg co-clusters. Data from recent literature is compared with predictions with the model. (HV data from [2, 17] is converted to yield strength, see text.)

To understand the novelty in the new model, it is particularly relevant to note that the present model predicts that the magnitude of the SRO strengthening effect due to co-clusters, which is the main strengthening mechanism in these alloys, is proportional to the amount of co-clusters formed. Thus the type of precipitation strengthening caused by co-clusters is very different from classical strengthening effects such as Orowan (precipitate by-passing) strengthening, strengthening by shearing of ordered precipitates and chemical strengthening, which all possess (in good approximation, for dilute alloys) a volume fraction to the power ½ dependency [19- 30]. This distinct difference with other precipitation hardening

mechanisms follows from the assumption that all enthalpy change is related to bonds of Cu–Mg pairs and that interaction with moving dislocations is determined exclusively by the breaking of this bond. As a result the distance between obstacles on a shear plane is small (typically $y_A^{-1/2}\, b$, i.e. about 10 b for alloys considered here) and the obstacle strength is low. In these conditions the classical approach based on bowing dislocations and their line tension, which leads to volume fraction to the power ½ dependency (see, e.g. [19]), is not valid, and is thus not applicable in the present model. To further verify this point, Fig. 6 shows a plot of the predicted volume fraction of co-clusters using the model in Section 2 versus measured proof strength data from the database described in [3] and Table 1. This figure confirms the linear proof strength – co-cluster volume relation, and clearly shows that the volume fraction to the power ½ dependency is not valid. (Note that due to smaller alloy-dependent strengthening effects such as solution strengthening and dispersion strengthening, data in Fig. 6 will not strictly lie on a single straight line.)

5. Conclusions

Predictions of a model for the thermodynamics of and strengthening due to Cu–Mg co-clusters in Al–Cu–Mg based precipitation hardening alloys have been compared with recent data on Al–Cu–Mg alloys aged to the hardness plateau studied by 3 dimensional atom probe, small angle X-ray scattering experiments (SAXS) and strength and hardness measurements. The predictions of strength are in excellent agreement with the measured data. Alloy strength is dominated by SRO strengthening which in good approximation increases linearly with co-cluster content. Data on Cu:Mg ratio in the co-clusters and the total amount of clusters are in good agreement with the model. The Guinier radius of the co-clusters as determined by SAXS is in good agreement with the model.

Acknowledgements

This paper was presented as an invited plenary lecture at the European Conference for Aluminium Alloys, October, 5-7, 2011, Bremen, Germany; the Deutsche Gesellschaft für Materialkunde (DGM) is gratefully acknowledged for providing funding for conference attendance. Dr Jialin Yan and Dr Nong Gao are acknowledged for additional DSC analysis.

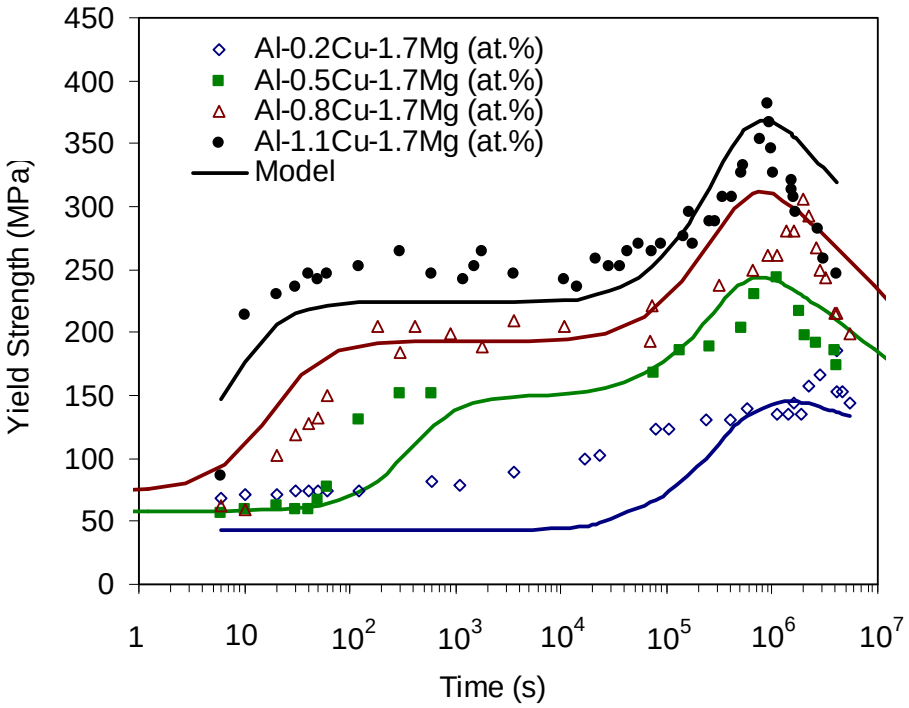

Figure 1:
Strength evolution for Al–*x*Cu–1.7Mg alloys (*x* = 0.2, 0.5, 0.8 and 1.1) (at.%) aged at 150 ºC. (Strength data converted from hardness data.) Data from [8]. (Lines are from a now partly obsolete model described in [9].)

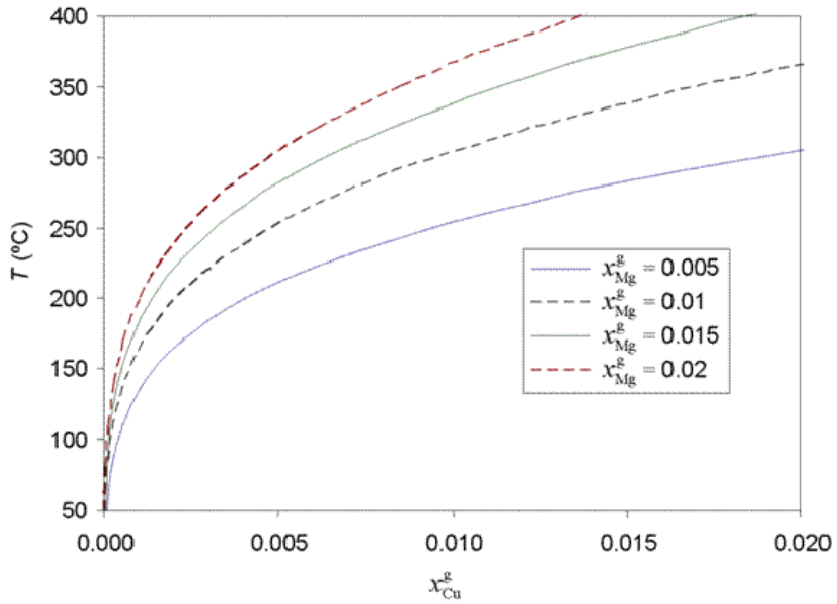

Figure 2:
Metastable solvi of Cu–Mg clusters in Al-rich ternary alloys for various Mg contents as calculated from the model. x^{g}_{Cu} is the gross Cu content of the alloy; x^{g}_{Mg} is the gross Mg content of the alloy.

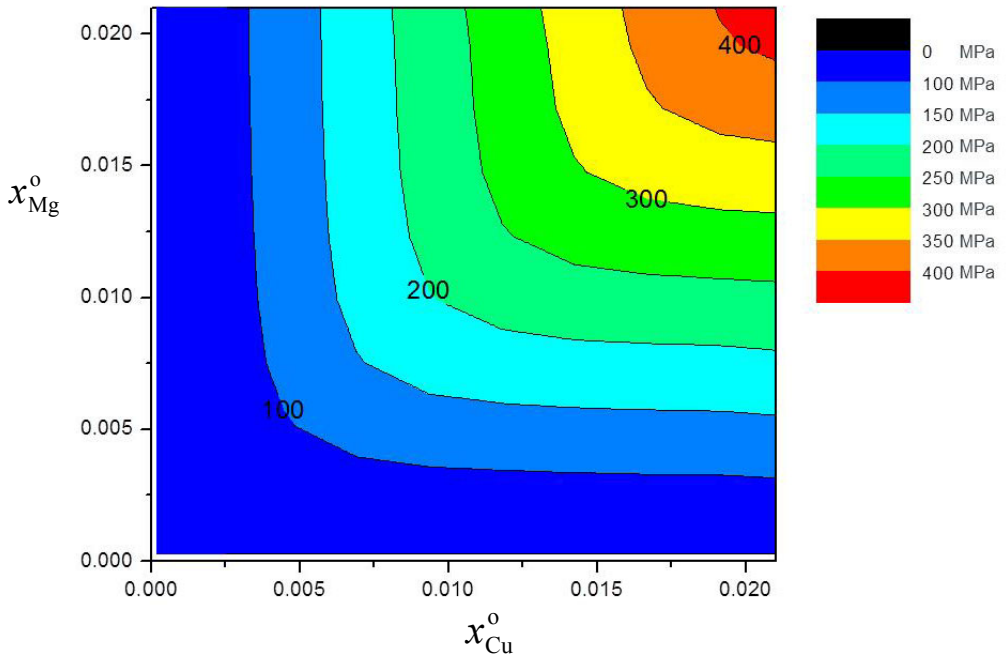

Figure 3:
Predicted proof strengths of Al–Cu–Mg based alloys aged at 120 °C to the strength plateau (full co-cluster formation). x^{o}_{Cu} and x^{o}_{Mg} refer to the amounts of Cu and Mg dissolved in the Al-rich phase after solutionising.

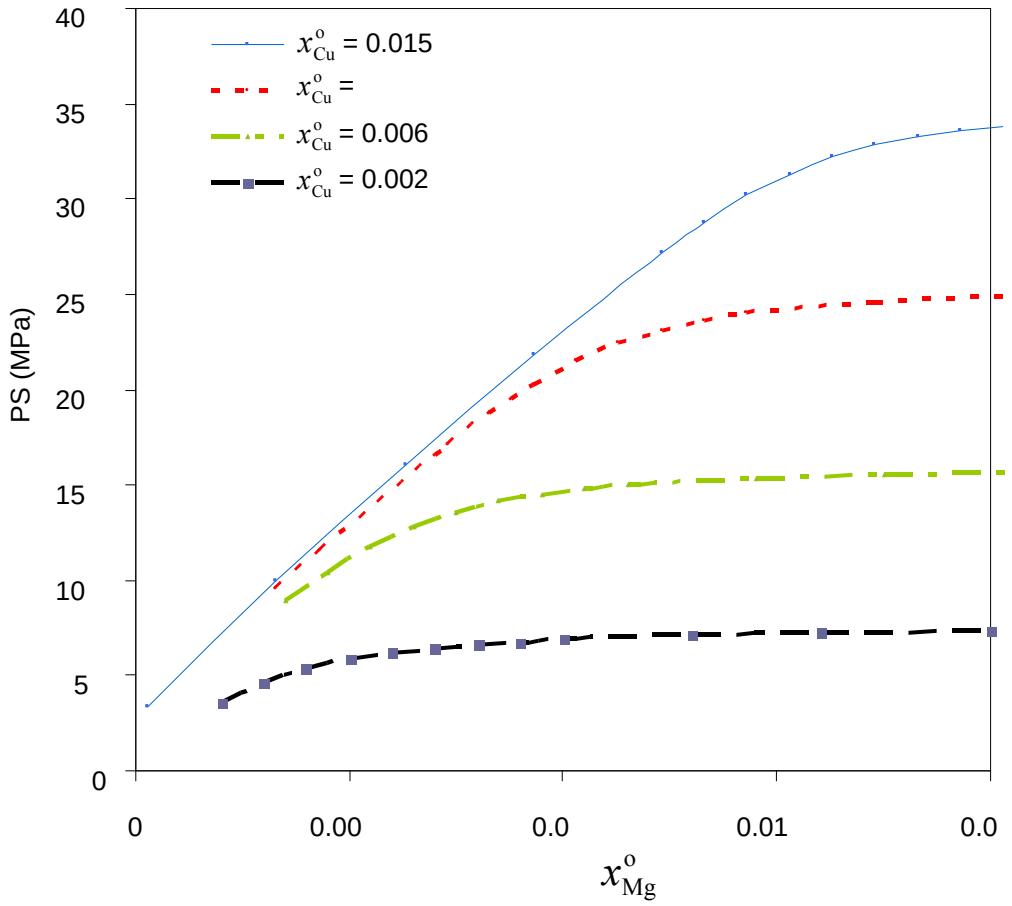

Figure 4:
Predicted proof strengths (PS) of Al–Cu–Mg based alloys aged at room temperature to the strength plateau (full co-cluster formation). x^{o}_{Cu} and x^{o}_{Mg} refer to the amounts of Cu and Mg dissolved in the Al-rich phase after solutionising.

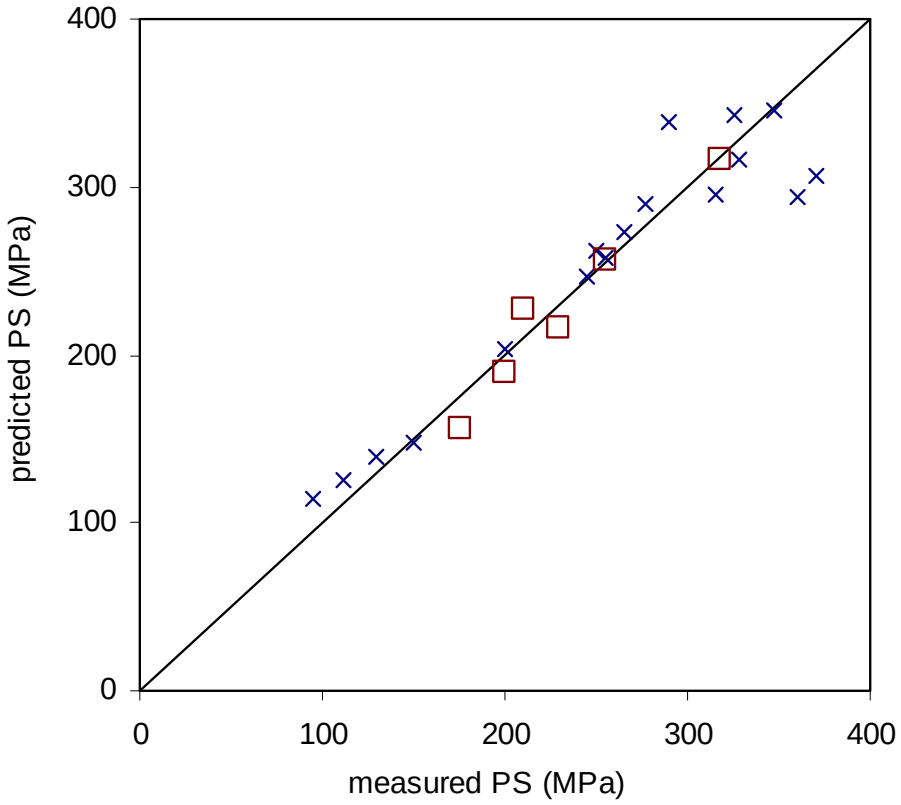

Figure 5:
Measured and predicted proof strengths (PS) of 23 Al–Cu–Mg based alloys aged to completion of co-cluster formation.
× data and alloys described in [3],
□ new data [2, 6, 17] on 6 alloys from Table 1.

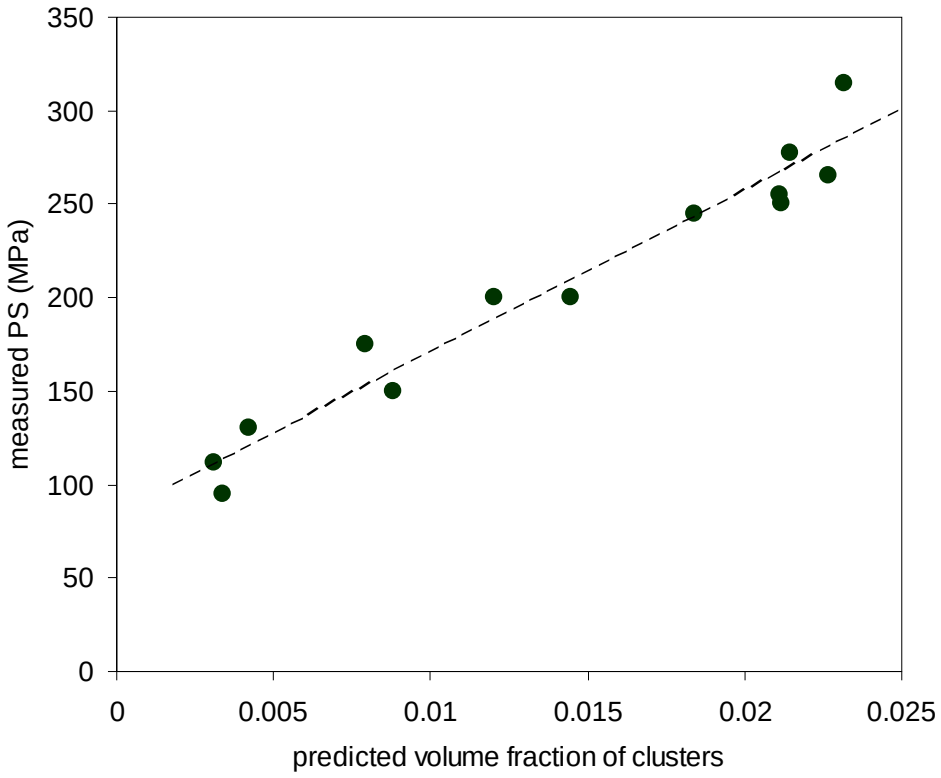

Figure 6:
Measured proof strengths (PS) of quenched and aged (non-stretched) Al–Cu–Mg based alloys aged to the strength plateau vs the predicted volume fraction of co-clusters. The linear dependency is consistent with the present co-cluster strengthening model.

References

[1] G. Sha, R.K.W. Marceau, X. Gao, B.C. Muddle, S.P. Ringer: Acta Mater. 59 (2011) 1659

[2] R.K.W. Marceau, G. Sha, R. Ferragut, A. Dupasquier, S.P. Ringer: Acta Mater. 58 (2010) 4923.

[3] M.J. Starink, S.C. Wang: Acta Mater. 57 (2009) 2376.

[4] A. Deschamps, T.J. Bastow, F. de Geuser, A.J. Hill, C.R. Hutchinson: Acta Mater. 59 (2011) 2918-2927.

[5] B. Klobes, K. Maier, T.E.M. Staab: Mater. Sci. Eng. A 528 (2011) p. 3253.

[6] K.D. Ralston, N. Birbilis, M. Weyland, C.R. Hutchinson: Acta Mater. 58 (2010) 5941.

[7] N. Kamp, N. Gao, M.J. Starink, I. Sinclair: Int. J. Fatigue 29 (2007) 869.

[8] K. Raviprasad, S. Moutsos, in: J.F. Nie, A.J. Morton, B.C. Muddle (Eds.), Proc 9th International Conference on Aluminium Alloys (ICAA9), 2004, Institute of Materials Engineering Australasia Ltd., Brisbane, Australia (2004) 412.

[9] J. Yan, N. Gao, M.J. Starink: Mater. Sci. Forum 28 (2004) 926.

[10] S.C. Wang, M.J. Starink, N. Gao: Scripta Mater. 54 (2006) 287.

[11] H. Shih, N. Ho, J.C. Huang: Metall Mater Trans A 27 (1996) 2479.

[12] S.C. Wang, M.J. Starink: Int Mater Rev. 50 (2005) 193.

[13] N.A. Belov, D.G. Eskin, A.A. Aksenov, Multicomponent Phase Diagrams, Elsevier, 2005.

[14] M.J. Starink, S.C. Wang: Scripta Mater. 62 (2010) 720-723.

[15] G. Kostorz, B. Schonfeld: Chimia 55 (2001) 517-522.

[16] M.J. Starink, N. Gao, L. Davin, J. Yan, A. Cerezo: Phil. Mag. 85 (2005) 1395.

[17] P. Jin, B.L. Xiao, Q.Z. Wang, Z.Y. Ma, Y. Liu, S. Li: Mater. Sci. Eng. A 528 (2011) 1504

[18] M.J. Starink, I. Sinclair, N. Gao, N. Kamp, P.J. Gregson, P. Pitcher, A. Levers, S. Gardiner: Mater. Sci. Forum, 396-402 (2002) 601.

[19] A.J. Ardell: Metall. Trans. A 16 (1985) 2131.

[20] L.M. Brown, R.K. Ham, in: A. Kelly, R.B. Nicholson (Eds.), Strengthening Methods in Crystals, Applied Science Publishers, London (1965) 9–135.

[21] I.N. Khan, M.J. Starink: Mater Sci Techn 24 (2008) 1403-1410

[22] C. Schlieser, E. Nembach. Acta Metall. Mater. 43 (1995) 3983.

[23] M.J. Starink, S.C. Wang: Acta Mater. 51 (2003) 5131-5150.

[24] V. Gerold, H.J. Gudladt, J. Lendvai: Physica status solidi (a) 131 (1992) 509.

[25] M.J. Starink, P. Wang, I. Sinclair, P.J. Gregson: Acta Materialia 47 (1999) 3855-3868.

[26] B.C. Lee, J.K. Park: Acta mater. 46 (1998) 4181.

[27] S.C. Wang, F. Lefebvre, J.L. Yan, I. Sinclair, M.J. Starink: Mater. Sci. Eng. A 431 (2006) 123-136

[28] A.W. Zhu, E.A. Starke: Acta Mater. 47 (1999) 3263.

[29] I.N. Khan, M.J. Starink, J.L. Yan: Mater. Sci. Eng. A 472 (2008) 66.

[30] L. Cartaud, J. Guillot, J. Grilhe, in: Proc. ICSMA IV, Vol. 1, Nancy, France (1976) 214.